# Interrogating Explicit Solvent Effects on the Mechanism and Site-Selectivity of Aryl Halide Oxidative Addition to $L_2Pd(0)$

Jingru Lu,[a] Holly Celuszak,[a] Irina Paci,*[a] and David C. Leitch*[a]

[a] Dr. J. Lu, H. Celuszak, Prof. Dr. I. Paci, Prof. Dr. D. C. Leitch
Department of Chemistry
University of Victoria
3800 Finnerty Rd., Victoria, BC V8P 5C2 (Canada)
E-mail: ipaci@uvic.ca; dcleitch@uvic.ca

**Abstract:** We report a study of solvent effects on the rate, selectivity, and mechanism of (hetero)aryl (*pseudo*)halide oxidative addition to $Pd(PCy_3)_2$ as an exemplar of $L_2Pd(0)$ species. First, 2-chloro-3-aminopyridine is observed to undergo faster oxidative addition in toluene compared to more polar solvents, which is not consistent with the trend we observe with many other 2-halopyridines. We attribute this to solvent basicity hydrogen-bonding between solvent and substrate. Greater hydrogen-bond donation from the substrate leads to a more electron-rich aromatic system, and therefore slower oxidative addition. We demonstrate how this affects rate and site-selectivity for hydrogen-bond donating substrates. Second, electron-deficient multihalogenated pyridines exhibit improved site-selectivity in polar solvents, which we attribute to different C–X sites undergoing oxidative addition by two different mechanisms. The C–X site that favours the more polar nucleophilic displacement transition state is preferred over the site that favours a less-polar 3-centered transition state. Finally, (hetero)aryl triflates consistently undergo faster oxidative addition in more polar solvents, which we attribute to highly polar nucleophilic displacement transition states. This leads to improved site-selectivity for C–OTf oxidative addition, even in the presence of highly reactive 2-pyridyl halides.

## Introduction

Selection of an appropriate solvent is one of the most important factors in reaction optimization in homogenous catalysis.[1–7] Solvent properties can significantly affect the rate and selectivity of a reaction, as well as the speciation, stability, and performance of a catalyst.[8–21] In palladium-catalyzed cross-couplings, solvent plays many roles in reaction outcomes.[22–24] An obvious factor is the solubility (or lack thereof) of the various reaction components. Mechanistically, polar solvent media can stabilize polar intermediates and/or transition states,[25] as well as affecting equilibria including the acidity/basicity of the reactants and reagents.[26–28] Solvent molecules can also directly participate in reaction mechanisms, for example by coordinating to a palladium center to change catalyst speciation and therefore rate/selectivity.[21,29,30]

In this work, we report how specific solvent effects influence the rate and site-selectivity of oxidative addition to Pd(0).[31–34] We use $Pd(PCy_3)_2$ as an exemplar system for a 14-electron $L_2Pd(0)$ species.[35,36] In a preceding paper,[37] we describe an expanded quantitative model for the oxidative addition of various substituted (hetero)aryl halides to $Pd(PCy_3)_2$ using three reaction solvents: toluene, THF and 1:1 DMF/THF. Under the conditions used, we observe only modest solvent effects on the oxidative addition free energies of activation ($\Delta G^{\ddagger}_{OA}$), meaning solvent identity is not a statistically significant descriptor for a linear regression model. In this work, we examine several subtle outliers to this general trend, and identify and elucidate solvent effects on the rate/selectivity of oxidative addition for specific substrate types. We describe three distinct categories of solvent effects (Fig. 1).

The first solvent effect category is related to the solvent hydrogen bonding basicity (SHBB, quantified by experimental $pK_{HB}$ values)[38] and its impact on the electronic properties of electrophiles able to participate as hydrogen-bond donors. An intermolecular H-bond between a solvent with a large $pK_{HB}$ (*e.g.* DMF) and a substrate carrying a strong hydrogen-bond donor (*e.g.* $–NH_2$) will increase the electron density around the reactive centre, resulting in a significant effect on both the reaction rate and site-selectivity of these substrates in oxidative addition (Fig. 1A).

The second category concerns the impact of solvent polarity on site-selectivity of specific 3-substituted-2,6-dichloropyridine derivatives. For substrates with an electron-withdrawing group (EWG) at the 3 position, the degree of $C_6/C_2$ selectivity is influenced by the fact that different oxidative addition reaction mechanisms operate based on frontier molecular orbital symmetries.[39] The $C_6$ site reacts via a polarized nucleophilic displacement transition state, while the $C_2$ site reacts via a relatively non-polar 3-centered transition state; accordingly, $C_6/C_2$ selectivity improves as solvent polarity increases (Fig. 1B).

The final category concerns oxidative addition of (hetero)aryl triflates. DFT calculations from previous work[14,21,37,40,41] reveal that oxidative addition of (hetero)aryl triflates to $L_2Pd(0)$ proceeds *via* a nucleophilic displacement pathway, leading to a highly polar transition state. This is consistent with our experimental observations that (hetero)aryl triflates react faster in polar solvents. Accordingly, solvent identity has a significant effect on the site-selectivity of 2-halopyridyl triflate derivatives, where using polar solvents improves site-selectivity for oxidative addition at the triflate site (Fig. 1C).

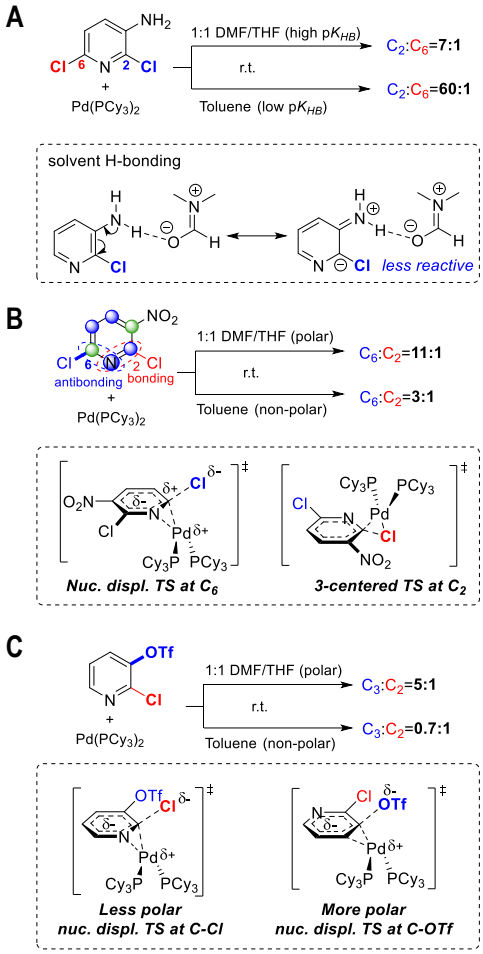


**Figure 1.** Summary of the solvent effect categories identified in this work. **(A)** Influence of solvent hydrogen bonding on oxidative addition outcomes, with the site-selectivity of 2,6-dichloro-3-aminopyridine as a representative example. **(B)** Solvent effects on site-selectivity where two distinct oxidative addition mechanisms operate, with 2,6-dichloro-3-nitropyridine as a representative example. **(C)** Solvent effects on oxidative addition site-selectivity between a triflate and a halide site, with 2-chloropyridyl-3-triflate as a representative example.

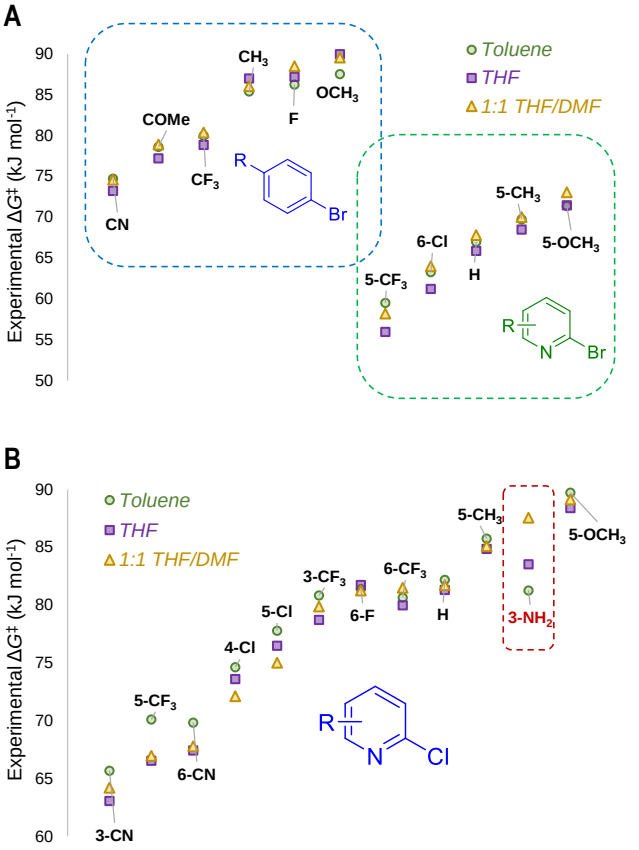


**Figure 2.** Experimental rates of the 11 overlapping (rates measured in all 3 solvents) (hetero)aryl bromides **(A)** and the 12 substituted 2-chloropyridines **(B)** oxidative addition to $Pd(PCy_3)_2$ in toluene, THF and 1:1 THF/DMF.[37]

## Results and Discussion

### Influence of Solvent Hydrogen Bond Basicity (p$K_{HB}$) on Oxidative Addition Rate and Site-Selectivity

As shown in Figure 2, oxidative addition of (hetero)aryl halides (Cl and Br) to $Pd(PCy_3)_2$ is slightly faster in THF and 1:1 THF/DMF compared to toluene, but overall these reactions have very similar experimental $\Delta G^{\ddagger}_{OA}$ values across the three solvents.[37] There is one exception – 2-chloro-3-aminopyridine – which reacts significantly faster in toluene ($\Delta G^{\ddagger}_{OA}$ = 81.3 kJ mol$^{-1}$) and in THF (83.5 kJ mol$^{-1}$) than in 1:1 THF/DMF (87.6 kJ mol$^{-1}$). This reversed reactivity trend and the significant differences among the measured $\Delta G^{\ddagger}_{OA}$ values in different solvents make this substrate a clear outlier from the overall (Het)Ar–Cl/Br data set.

Based on many published mechanistic studies, there are two general mechanisms for oxidative addition of Ar–X substrates to Pd(0): a relatively non-polar 3-centered insertion mechanism[42–46] is common for halobenzenes and iodide-based substrates, and a more polar nucleophilic displacement mechanism[39,41,46–48] is generally favoured for 2-halopyridines. The specific mechanism of 2-chloro-3-aminopyridine oxidative addition to $Pd(PCy_3)_2$ has been previously investigated as part of our study of the frontier molecular orbital effects on oxidative addition mechanisms, with the nucleophilic displacement mechanism favoured due to *LUMO* symmetry.[39] Figure 3 shows how high *LUMO* density at $C_2$ and a π-antibonding relationship between $C_2$ and $N_1$ favours coordination of both atoms Pd *via* the *HOMO*-1 of $Pd(PCy_3)_2$.

As the nucleophilic displacement transition state is more polar than a 3-centered transition state, polar solvents should *accelerate* oxidative addition for this substrate; however, 2-chloro-3-aminopyridine is more reactive in *less* polar solvents (toluene > THF > THF/DMF), which indicates solvent properties other than polarity may be responsible. Given the structure of the substrate, we hypothesized that SHBB[38] could be the primary factor for the observed reactivity differences in these three solvents. The solvent-solute hydrogen bond (H-bond) interaction plays an important role in determining a wide range of chemical properties, and myriad studies have been done to understand its impact in various molecular systems and reactions.[49–57] Relevant to this work, Wang and coworkers reported a dramatic effect of SHBB on the regioselectivity of $S_NAr$ reactions.[58] In organopalladium chemistry, Xiao and coworkers reported that solvent-substrate

hydrogen bonding can enhance the rate of aryl chloride oxidative addition through H-bond *donation* by ethylene glycol to the chloride;[59] however, to the best of our knowledge, SHBB has not been studied as a rationale for rate and/or selectivity in oxidative addition to Pd(0).

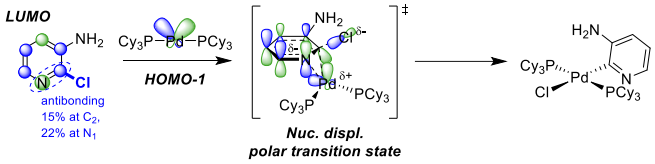


**Figure 3** Oxidative addition of 2-chloro-3-aminopyridine to $Pd(PCy_3)_2$ via the nucleophilic displacement mechanism and the key frontier orbitals involved.[39]

To probe if SHBB is a factor in the oxidative addition of 2-chloro-3-aminopyridine, we examined other substrates with H-bond donors (Fig. 4). Using the same competition experiment approach we applied to our prior work,[37,48,60] we measured $\Delta G^{\ddagger}_{OA}$ values for the oxidative addition of 2-chloro-3-hydroxypyridine in different solvents (Fig. 4A). These $\Delta G^{\ddagger}_{OA}$ values are 79.9 kJ mol$^{-1}$ in toluene, 82.1 kJ mol$^{-1}$ in THF, and 91.9 kJ mol$^{-1}$ in DMF/THF, following the same trend as for the 3-$NH_2$ derivative. In contrast, unsubstituted 2-chloropyridine has nearly identical $\Delta G^{\ddagger}_{OA}$ values in all three solvents (82.2, 81.3, and 81.7 kJ mol$^{-1}$ respectively).

Solvents with higher $pK_{HB}$ values are better H-bond acceptors, with $pK_{HB}$(THF) = 1.26 and $pK_{HB}$(DMF) = 2.06. The intermolecular interaction between these solvent molecules and a substrate containing an H-bond donor will distort the electron density of the substrate, affecting its reactivity. The calculated structure of 2-chloro-3-aminopyridine with one explicit DMF molecule has the carbonyl oxygen acting as an H-bond acceptor from the –$NH_2$ group (Fig. 4B). This will generate partial negative charge at the amino nitrogen, turning it into a stronger EDG and thus deactivating the substrate toward oxidative addition.

To quantitatively account for the SHBB on the electronic features of these substrates, we performed DFT calculations on each 2-Cl-3-Z-pyridine (Z = $NH_2$, OH, H) in the absence and presence of one explicit solvent molecule (THF or DMF). For each structure, the implicit CPCM solvation model was also applied to account for solvent dielectric effects. To generate the H-bonded complexes, the initial geometry contains the substrate and one solvent molecule, with the atoms acting as H-bond donor and acceptor placed close to each other. Optimized structures and energies for the H-bonded complexes were obtained at the B3LYP/def2-TZVPD//B3LYP/def2-SVP level of theory.

Solvent hydrogen bond effects can be evaluated from these H-bonded structures using calculated molecular electrostatic potentials (*ESP*)[61] at the $C_2$ sites of the 3-amino and 3-hydroxy derivatives, along with the unsubstituted 2-chloropyridine as a comparator (Fig. 4C). The $\Delta ESP_{C2}$ values shown are calculated as the difference between the $ESP_{C2}$ of the substrate-solvent H-bonded complex and the $ESP_{C2}$ of the substrate itself (both calculated using CPCM implicit solvation). This ensures $\Delta ESP_{C2}$ only accounts for the influence from the substrate-solvent H-bond. In all cases, the presence of the explicit solvent molecule leads to larger negative *ESP* at the $C_2$ site, corresponding to increased electron density. Comparing the $\Delta ESP_{C2}$ of the 3-$NH_2$ and 3-OH derivatives to 2-chloropyridine, there is clearly a greater electronic effect at the $C_2$ site when the solvent-substrate H-bond is present. A plot of the *ESP* isosurfaces for 2-chloro-3-aminopyridine and its H-bonded complex with DMF provides a direct visualization of the H-bonding effect on the electron density around the pyridyl ring (Fig. 4D).

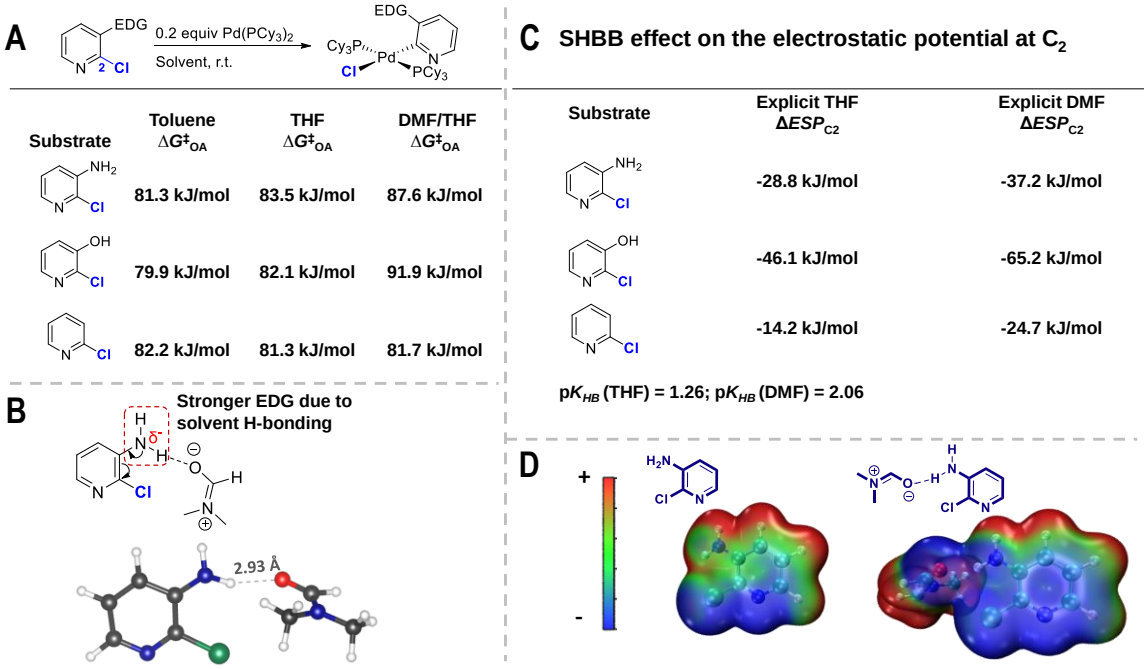


**Figure 4. (A)** Experimental $\Delta G^{\ddagger}_{OA}$ for oxidative addition of 2-chloro-3-aminopyridine, 2-chloro-3-hydroxypyridine and 2-chloropyridine to $Pd(PCy_3)_2$ in toluene, THF and 1:1 THF/DMF. **(B)** Calculated structure and schematic of intermolecular H-bond between DMF and the –$NH_2$ group, and its deactivating effect on the $C_2$ site. **(C)** Computational analysis of the solvent hydrogen bond basicity (SHBB) effect on the calculated *ESP* at the $C_2$ site; $\Delta ESP_{C2}$ values are the difference between $ESP_{C2}$ of the substrate-solvent H-bond complex in the CPCM solvation model and $ESP_{C2}$ of the substrate itself in the CPCM solvation model. **(D)** *ESP* isosurfaces at 0.002 au of 2-chloro-3-aminopyridine and the 2-chloro-3-aminopyridine–DMF H-bond complex; blue represents negative *ESP*, and red represents positive *ESP*.

Notably, our prior work on quantitative structure-reactivity relationships for (Het)Ar–X oxidative addition to $Pd(PCy_3)_2$ indicates that the *ESP* at the reactive carbon is the highest contributing descriptor to the MLR models, where larger positive values correlate strongly with faster OA reactions, and larger negative values correlate with slower OA reactions.[37,48] The $\Delta ESP_{C2}$ trends from Figure 4C are therefore entirely consistent with the expected reactivity trends from these prior MLR models.

The structures of both the substrate and the solvent impact the $\Delta ESP_{C2}$ values. There is a clear trend toward larger negative $\Delta ESP_{C2}$ for structures in DMF than those in THF by 10–20 kJ mol$^{-1}$. Some of this change is clearly due to solvent dielectric effects, as the $\Delta ESP_{C2}$ for simple 2-chloropyridine is also -10 kJ mol$^{-1}$; however, for 2-chloro-3-hydroxypyridine in DMF, the $\Delta ESP_{C2}$ is -65 kJ mol$^{-1}$, nearly 20 kJ mol$^{-1}$ more negative than the corresponding structure in THF.

To highlight substrate structure effects, we consider the THF series as an example: For 2-chloropyridine, the distance between the oxygen of the THF and the $C_3$–H is 2.3 Å. This weak interaction is consistent with the low $\Delta ESP_{C2}$ (-14.2 kJ mol$^{-1}$). A distance of 1.9 Å between the oxygen of THF and the N–H of the 3-$NH_2$ derivative, and a larger $\Delta ESP_{C2}$ value, indicate a stronger H-bond interaction. For the 3-OH derivative, the $O_{THF}$ to H–OPy distance is only 1.6 Å, and the $\Delta ESP_{C2}$ (-46.1 kJ mol$^{-1}$) is the largest among the three substrates. Here, the considerably more acidic hydroxyl proton results in a stronger solvent-substrate H-bond interaction. This is consistent with the 2-chloro-3-hydroxylpyridine experiencing a larger range of $\Delta G^{\ddagger}_{OA}$ values from toluene to DMF/THF (79.9 – 91.9 kJ mol$^{-1}$) compared to the 3-amino derivative (81.3 – 87.6 kJ mol$^{-1}$).

Importantly, the proposed solvent H-bond effect is also consistent with observed oxidative addition site-selectivity for three 2,6-dichloro-3-EDG-pyridine derivatives (EDG = $NH_2$, NHAc and OH, Fig. 5). Comparing the measured site-selectivity in different solvent systems, one can observe a clear trend that the best $C_2/C_6$ selectivity is achieved in toluene, a low $pK_{HB}$ solvent. As the (co-)solvent $pK_{HB}$ increases, there is a consistent decrease to the $C_2/C_6$ selectivity with all three substrates. Further experimental evidence of this solvent H-bond effect is given by the site-selectivity data of the 3-OMe and 3-OAc derivatives in different solvents: for the two substrates carrying no H-bond donor substituents, the $C_2/C_6$ selectivity remains unchanged ($C_2/C_6$ > 99:1 for 3-OMe and $C_2/C_6$ = 1:1 for 3-OAc) across the 3 solvent systems. This observation is in clear contrast to the 3-OH derivative case, where we observed a decrease in $C_2/C_6$ selectivity from 30:1 to 6:1 as the $pK_{HB}$ of the (co-)solvent increases. Unfortunately, attempts to invert the selectivity through the use of other H-bond acceptors (DMA, $NEt_3$) were not successful.

If substrate-solvent H-bonding is responsible for making H-bond donating groups more electron-donating, this should deactivate both $C_2$ (*ortho*) and $C_6$ (*para*) sites through resonance; this is not consistent with the decreased $C_2/C_6$ selectivity, which suggests the deactivating effect at $C_2$ is more pronounced. We therefore examined the effect on *ESP* values for the $C_2$ and $C_6$ positions *via* DFT calculations (conducted in the same way as for the 2-chloro-3-EDG-pyridine derivatives discussed above). Electrostatic potential maps show that both sites are in fact deactivated by the solvent H-bond, as indicated by the highly

**A**

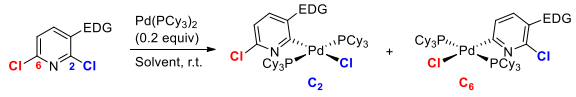


| Entry | Solvent | EDG = $NH_2$ $C_2$:$C_6$ | EDG = NHAc $C_2$:$C_6$ | EDG = OH $C_2$:$C_6$ | EDG = OMe $C_2$:$C_6$ | EDG = OAc $C_2$:$C_6$ |
|---|---|---|---|---|---|---|
| 1 | Toluene | 60:1 | 80:1 | 30:1 | >99:1 | 1:1 |
| 2 | THF | 9:1 | 8:1 | 6:1 | >99:1 | 1:1 |
| 3 | 1:1 THF/DMF | 7:1 | 2:1 | 6:1 | >99:1 | 1:1 |
| 4 | 1:1 THF/DMA | 6:1 | -- | -- | -- | -- |
| 5 | 1:1 THF/$Et_3N$ | 4:1 | -- | -- | -- | -- |

**B** **SHBB effect on the *ESP* at $C_2$ and $C_6$**

| Substrate EDG = | No solvent H-bond | Explicit THF | Explicit DMF |
|---|---|---|---|
| | $\Delta ESP$ ($C_2$ - $C_6$) (kJ mol$^{-1}$) | | |
| $NH_2$ | 24.6 | 19.5 | 10.7 |
| NHAc | 18.0 | 7.5 | -9.0 |
| OH | 0.6 | -7.3 | -12.9 |

**C**

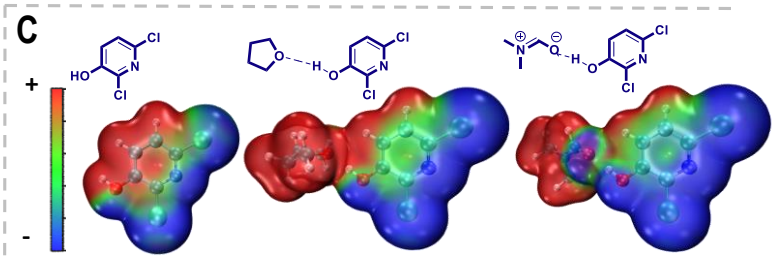


**Figure 5. (A)** Experimental $C_2/C_6$ selectivity for oxidative addition of 2,6-dichloro-3-EDG-pyridines (EDG = $NH_2$, NHCOMe, OH, OMe and OAc) to $Pd(PCy_3)_2$ in different solvents (>99:1 indicates only $C_2$ is observed by $^{31}P$ NMR spectroscopy). **(B)** Computational analysis of the solvent hydrogen bond basicity (SHBB) effect on the electrostatic potential (*ESP*) at the $C_2$ and $C_6$ sites; $\Delta ESP$ ($C_2$ - $C_6$) = $ESP_{C2}$ – $ESP_{C6}$. **(C)** *ESP* isosurfaces at 0.002 a.u. of 2,6-dichloro-3-hydroxypyridine, the substrate–THF complex, and the substrate–DMF complex; blue represents negative *ESP*, and red represents positive *ESP*.

negative electrostatic potential region around the reactive sites when an explicit solvent molecule is involved (Fig. 5C). However, quantitative analysis of the *ESP* values indicates that the $C_2$ sites are deactivated to a greater degree than the $C_6$ sites in all cases: the difference between the *ESP* values at $C_2$ and $C_6$ decreases as SHBB increases (Fig. 5B). This is consistent with the observed decrease in $C_2$ selectivity in solvents with high p$K_{HB}$.

In summary, solvent hydrogen bond basicity (p$K_{HB}$) influences the rate and selectivity of oxidative addition for substrates containing a hydrogen bond donor functional group. Intermolecular H-bonding between solvents with high p$K_{HB}$ and substituents like -$NH_2$, -NHCOMe and -OH increases the electron density of the pyridine rings, and results in a strong deactivating effect toward oxidative addition reactivity. This effect also alters the site-selectivity of 2,6-dichloro-3-EDG-pyridines, where the best $C_2/C_6$ selectivity occurs in toluene, following a trend that solvents with high p$K_{HB}$ give lower $C_2/C_6$ selectivity. Computational analysis supports this experimental observation by showing how the solvent H-bond with the EDGs at the $C_3$ position deactivates the $C_2$ site more strongly than the $C_6$ site.

## Influence of Solvent Polarity on Oxidative Addition Site-Selectivity

In addition to solvent effects on the oxidative addition of EDG-substituted 2-chloropyridines discussed above, we studied oxidative addition site-selectivity as a function of solvent identity for several electron-deficient dichloropyridines (Fig. 6). The three 2,6-dichloro-3-EWG-pyridines (EWG = CN, $NO_2$, CHO) shown were previously investigated in our frontier molecular orbital study: with $Pd(PCy_3)_2$, $C_6$ and $C_2$ sites favour different mechanisms (nucleophilic displacement and 3-centered, respectively) due to the *LUMO* symmetry. This leads to $C_6$ as the major site for oxidative addition in THF.[39]

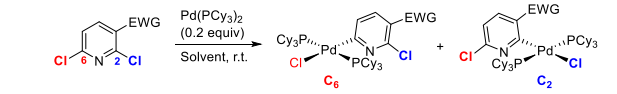


| | | EWG = CN | EWG = $NO_2$ | EWG = CHO |
|---|---|---|---|---|
| **Entry** | **Solvent** | **$C_6$:$C_2$** | **$C_6$:$C_2$** | **$C_6$:$C_2$** |
| 1 | Toluene | 5:1 | 3:1 | >> |
| 2 | THF | 10:1 | 7:1 | >> |
| 3 | 1:1 THF/DMF | 10:1 | 11:1 | >> |
| 4 | 1:1 THF/MeOH | -- | 10:1 | -- |

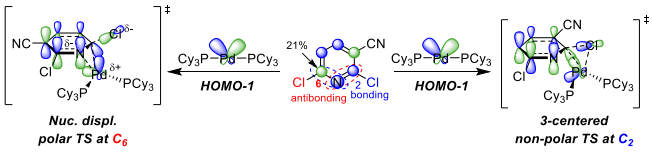


**Figure 6.** Observed $C_6/C_2$ selectivity of 2,6-dichloro-3-EWG-pyridines (EWG = CN, $NO_2$, CHO) in different solvents, and proposed hypothesis that the increased $C_6/C_2$ selectivity in polar solvents is caused by change in mechanism at the two sites.[39]

By examining the effect solvent identity has on site-selectivity, we observe that the 3-CN and 3-$NO_2$ derivatives have good $C_6/C_2$ selectivity (~10:1) in solvents with high dielectric constants (THF, 1:1 mixtures of THF/DMF and THF/MeOH), while the ratios between the $C_6/C_2$-isomers drop to 5:1 (3-CN) and 3:1 (3-$NO_2$) in toluene. These observations are consistent with the proposed change in reaction mechanism between the two sites, where oxidative addition at $C_6$–Cl proceeds through a polar nucleophilic displacement pathway, whereas reaction at $C_2$ proceeds through a non-polar 3-centered mechanism. Higher polarity solvents will stabilize the polar nucleophilic displacement transition state, resulting in faster oxidative addition at $C_6$. This observed solvent effect on $C_6/C_2$ selectivity provides additional experimental evidence in support of our mechanistic hypothesis that the $C_2$–Cl and $C_6$–Cl sites undergo oxidative addition by different mechanisms.

Notably, 3-formyl-2,6-dichloropyridine exhibits excellent $C_6/C_2$ selectivity (>99:1) in all solvent systems, regardless of the solvent dielectric constant. A possible reason for solvent polarity not having a significant influence on site selectivity is that this substrate is intrinsically heavily biased toward oxidative addition at $C_6$. Our *ESP*-based prediction model from our previously published work[48] predicts high $C_6/C_2$ selectivity ($\Delta\Delta G^{\ddagger}_{OA}$ = 6.8 kJ $mol^{-1}$) for the 3-CHO derivative, but only moderate to poor selectivity for the 3-CN and 3-$NO_2$ derivatives ($\Delta\Delta G^{\ddagger}_{OA}$ = 0.0 kJ $mol^{-1}$ and 3.4 kJ $mol^{-1}$, respectively).[62] The smaller $\Delta\Delta G^{\ddagger}_{OA}$ values for 3-CN and 3-$NO_2$ indicate that the electronic differentiation of these two sites is less pronounced; as a result, other reaction parameters, such as solvent polarity, are likely to exert an observable effect on site-selectivity.

## Solvent Effects on Aryl Triflate Oxidative Addition and Site-Selectivity with $Pd(PCy_3)_2$

One substrate class where we observe a clear trend between solvent identity and experimental oxidative addition rate is for aryl triflates. Comparing $\Delta G^{\ddagger}_{OA}$ values for a series of eight aryl triflates in the three solvent systems reveals that oxidative addition is consistently faster as the solvent polarity increases (Fig. 7A, data from ref. [37]). In addition, there are much larger differences between the $\Delta G^{\ddagger}_{OA}$ values of the same substrate measured in different solvents relative to other substrate types. The average difference between $\Delta G^{\ddagger}_{OA}$(toluene) and $\Delta G^{\ddagger}_{OA}$(DMF/THF) is 5.0 kJ $mol^{-1}$ (nearly a factor of 10 in rate at room temperature) for the aryl triflates; in contrast, the average $\Delta G^{\ddagger}_{OA}$ difference for the (hetero)aryl bromides in Figure 2 is only 0.7 kJ $mol^{-1}$.

We propose that these Ar–OTf substrates undergo oxidative addition to $Pd(PCy_3)_2$ *via* a polar nucleophilic displacement mechanism. Hammett plots for this substrate set in each solvent system yield nearly identical reaction constants, ρ = 3.7 (toluene and THF/DMF) and 3.9 (THF), consistent with a polar mechanism (Fig. 7B). Notably, these values are higher than that obtained by Jutand and Mosleh for oxidative addition of a similar series of ArOTf substrates to $Pd(PPh_3)_4$ in DMF (ρ = 2.6),[63] and more in-line with those obtained by Maes and Jutand for oxidative addition of 2-Cl-5-Z-pyridines using $Pd(PPh_3)_4$ ($\rho_{THF}$ = 4.3 and $\rho_{DMF}$ = 3.9);[46] these latter substrates are proposed to undergo oxidative addition *via* a nucleophilic displacement mechanism. Furthermore,

prior computational studies by several research groups, including those of Houk, Schoenebeck, and Neufeldt, indicate that aryl triflates undergo oxidative addition to $L_2Pd(0)$ through a polar, nucleophilic displacement mechanism, with long Pd---OTf distances in the transition state.[14,40,41]

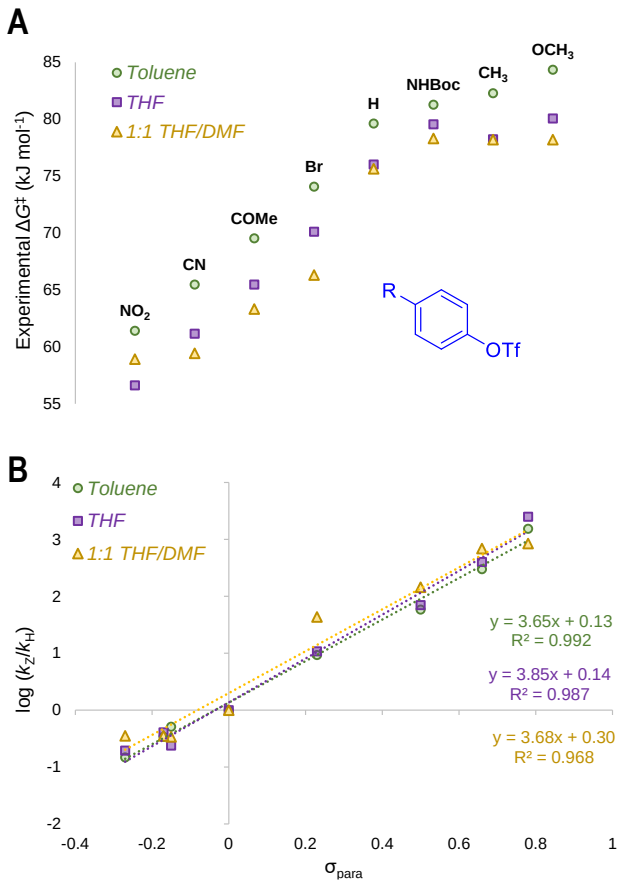


**Figure 7. (A)** Experimental rates of oxidative addition for eight para-substituted aryl triflates reacting with $Pd(PCy_3)_2$ in toluene, THF and 1:1 THF/DMF. **(B)** Corresponding Hammett plots. Data from ref. [37]

The greater charge separation in a nucleophilic displacement transition state is consistent with the observed solvent effect, where a polar transition state would be stabilized to a greater extent in polar solvents; however, other substrates that proceed *via* nucleophilic displacement should also exhibit this effect. The series of 2-halopyridines shown in Figure 2 clearly do not, despite the fact that many of these are also likely to undergo a nucleophilic displacement oxidative addition. To reconcile this, we examined the features of two calculated nucleophilic displacement transition states for the oxidative addition of 2-X-pyridine (X = Cl, OTf) (Fig. 8). We chose 2-pyridyl triflate for this comparison to maintain consistency with respect to the arene structure.

As described in prior work, 2-chloropyridine and 2-pyridyl triflate are both proposed to undergo oxidative addition to $Pd(PCy_3)_2$ *via* nucleophilic displacement, with the former passing through a polar transition state with Pd---$N_{ortho}$ bonding,[41,46,48] and the latter through an analogous transition state but with Pd---$C_{ortho}$ bonding.[37] In both cases, there is considerable partial positive charge on the Pd center, as well as partial negative charge delocalized throughout the pyridine ring; however, the magnitude of these charges is higher in the C–OTf oxidative addition transition state. The pyridyl group is 0.2*e* more negative and the Pd center is 0.06*e* more positive for C–OTf addition than for C–Cl (Hirshfeld charges). Furthermore, there is a greater increase in *ESP* at Pd from $Pd(PCy_3)_2$ to the transition structure for addition of the triflate versus the chloride, with an increase of 139 kJ $mol^{-1}$ versus 86 kJ $mol^{-1}$ respectively. These calculations are consistent with – at least in this case – (hetero)aryl triflate oxidative addition proceeding through a more polar transition state, which would be stabilized to a greater extent by polar solvents. However, other explanations are possible, such as changes to Pd(0) speciation (*vide infra*), and/or greater product stabilization of ionic $[L_2Pd(Ar)]^+[OTf]^-$ species in polar solvents (more exothermic oxidative addition and therefore faster rates by the Bell-Evans-Polanyi principle[64,65]). Jutand and Mosleh previously observed through conductivity studies that polar solvents (specifically, DMF and THF) lead to charge-separated oxidative addition products $[(Ph_3P)_2Pd(Ar)]^+$ $[OTf]^-$, whereas halide-containing oxidative addition products are neutral.[63]

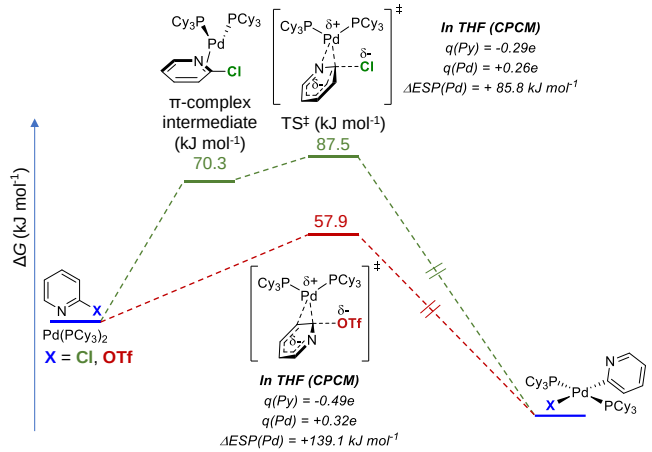


**Figure 8.** Transition state comparison for 2-X-pyridine (X = Cl, OTf) oxidative addition to $Pd(PCy_3)_2$ in THF (CPCM). *q*(Py) and *q*(Pd) are Hirshfeld charges at the indicated atoms, and Δ*ESP*(Pd) is the difference in molecular electrostatic potential at Pd between the transition state and $Pd(PCy_3)_2$.

Several research groups have studied the differences between oxidative addition of aryl triflates and other Ar–X electrophiles. These studies focus on how Pd(0) speciation – affected by both ligand *and* solvent – influences the preference for C–X (X = Cl, Br) or C–OTf oxidative addition. This is especially important for site-selective and/or iterative cross-coupling, which can be achieved by using different (*pseudo*)halide leaving groups.

In a seminal cross-coupling study, Littke and Fu reported ligand-controlled site-selectivity for the Suzuki coupling of 4-chlorophenyl triflate with 2-methylphenylboronic acid, observing that $PCy_3$ favours the C–OTf site while P(*t*-Bu)$_3$ favours the C–Cl site.[66] Subsequent computational work from Schoenebeck and Houk rationalized this selectivity change as a result of catalyst speciation, where 14-electron $L_2Pd(0)$ favours oxidative addition at the C–OTf site, whereas 12-electron LPd(0) favours oxidative

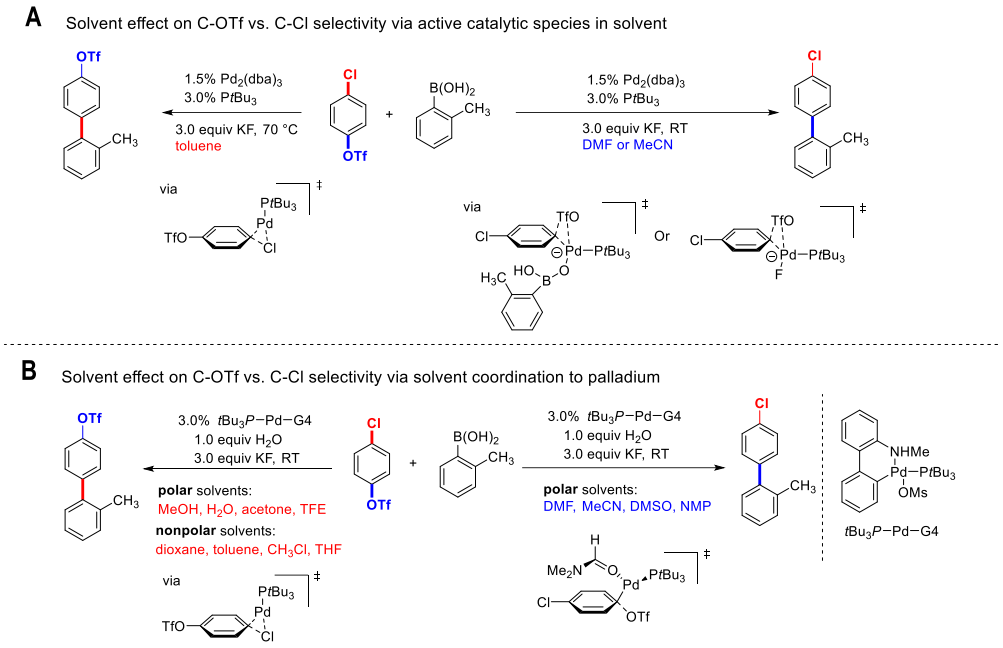


**Figure 9.** Previously reported solvent effects on C–OTf vs. C–Cl cross-coupling selectivity. **(A)** Selectivity for C–OTf increased with more polar solvents by favouring anionic palladate intermediates.[14] **(B)** Selectivity for C–OTf increased with more coordinating solvents by favouring 14-electron LPd(solvent) intermediates.[68]

addition of the C–Cl site.[40] Sigman and coworkers later reinforced this explanation on the basis of phosphine ligand descriptors.[67]

Solvent effects on the site-selectivity of this same Suzuki coupling catalyzed by Pd/P(*t*Bu)$_3$ were then investigated by Proutiere and Schoenebeck (Fig. 9A).[14] They found that C–Cl is the exclusive reacting site in less polar solvents (toluene and THF). In contrast, polar solvents reverse the site-selectivity, and high selectivity at the C–OTf site is observed in DMF and MeCN. Computational studies revealed that the selectivity is controlled by catalyst speciation, which changes depending on the solvent. In polar solvents, Pd[P(*t*Bu)$_3$] coordinates to anions in the reaction system to form 14-electron palladate species [Pd(P*t*Bu$_3$)X]$^-$ (X = F or ArBO$_2$H), which prefers C–OTf insertion via a lower energy transition state.

In 2022, Neufeldt and coworkers[21] investigated the same Suzuki coupling reaction with a wider range of solvents, and proposed that the solvent effect on catalyst speciation arises from solvent coordination to palladium (Fig. 9B). They observed that polar solvents including MeCN, DMF and DMSO favour reaction at the C–OTf bond, as observed by Proutiere and Schoenebeck; however, in other polar solvents like MeOH, acetone and H$_2$O, the major product is from C–Cl substitution. They re-evaluated the transition state energies using methods including dispersion correction, and the results suggest that instead of solvent polarity, the dramatic difference in site-selectivity is caused by the solvent coordinating ability. In coordinating solvent like DMF or MeCN, the reaction is catalyzed by 14-electron Pd[P(*t*Bu)$_3$](solvent), and the solvent-coordinated transition state for the rate-limiting oxidative addition is lower in energy for C–OTf insertion.

Notably, all of these prior studies indicate that *oxidative addition of C–OTf sites is favoured from 14-electron Pd(0) intermediates*, whether L$_2$Pd (*e.g.* Pd(PCy$_3$)$_2$), [LPdX]$^-$, or LPd(solvent). That these bisligated Pd(0) species favour C–OTf oxidative addition is consistent with the higher nucleophilicity of the more electron-rich Pd center interacting with the more electrophilic C–OTf site.[40] It is also consistent with Ar–OTf oxidative addition proceeding *via* the more polar, nucleophilic displacement mechanism.[44,46] The *HOMO*-1 of L$_2$Pd(0) (which becomes the *HOMO* as linear L–Pd–L is distorted to $C_{2v}$ symmetry) is symmetry matched to overlap with a π-antibonding unit in the electrophile *LUMO* adjacent to the C–OTf group.[47]

In our case, solvent effects on palladium speciation are less likely as an explanation for the lower $\Delta G^{\ddagger}_{OA}$ of Ar–OTf electrophiles in polar solvents. Since we are studying stoichiometric oxidative addition rather than catalytic coupling, no added anion sources are present. Furthermore, solvent coordination to Pd(PCy$_3$)$_2$ complex should be disfavoured due to the steric hindrance, and would also generate a less reactive trisligated, 16-electron Pd(0) species. While it is possible that a coordinating solvent like DMF could displace one of the PCy$_3$ ligands to generate a more reactive 14-electron Pd(0) species, it is not clear why this intermediate would exhibit faster oxidative addition rates only for Ar–OTf substrates and not other (hetero)aryl halides. However, at present we cannot rule out solvent-induced Pd(0) speciation changes as contributing to the solvent effect shown in Figure 7.

To further examine solvent effects on (hetero)aryl triflate oxidative addition, we studied site-selective C–OTf versus C–Cl or C–Br oxidative addition with the five substrates in Table 1. For 2-chloro-5-triflatopyridine and 2-chloro-6-triflatopyridine, oxidative addition to Pd(PCy$_3$)$_2$ takes place exclusively at triflate regardless of the solvent, even though the 2-chloro position is more reactive than a typical Ar–Cl (entries 2 and 3). In contrast, site-selectivity for 2-chloropyridin-3-yl-triflate is much lower and also influenced by solvent (entry 1). In polar solvent mixtures, oxidative addition

is favoured at the C–OTf site over the C–Cl site (5:1); however, this is reduced in THF (2:1) and even slightly inverted (1:1.3) in toluene (entry 1).

**Table 1.** Experimental site-selectivity for oxidative addition of C–OTf versus C–Cl or C–Br to $Pd(PCy_3)_2$ in multiple solvent systems.

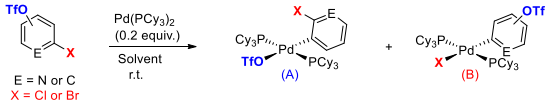


| | | Experimental Ratio **(A)** (OTf) **:** **(B)** (Cl/Br) | | | | |
|---|---|---|---|---|---|---|
| **Entry** | **Substrate** | **1:1 MeOH/THF** | **1:1 DMSO/THF** | **1:1 DMF/THF** | **THF** | **Toluene** |
| 1 |  | 5:1 | 5:1 | 5:1 | 2:1 | 1:1.3 |
| 2 |  | -- | > 99:1 | > 99:1 | > 99:1 | > 99:1 |
| 3 |  | -- | -- | > 99:1 | > 99:1 | > 99:1 |
| 4 |  | > 99:1 | > 99:1 | > 99:1 | > 99:1 | > 99:1 |
| 5 |  | 2:1 | 2:1 | 2:1 | 1:2 | 1:7 |

For triflate versus bromide selectivity, Wang and coworkers demonstrated ligand controlled selectivity in Pd-catalyzed Suzuki coupling.[68] Analogous to Littke and Fu's work, bulky $P(tBu)_3$ leads to reaction at bromide while the smaller $PPh_3$ leads to reaction at triflate. This is again consistent with 12-electron Pd[$P(t\text{-}Bu)_3$] favouring a 3-centered mechanism at C–Br, whereas 14-electron $Pd(PPh_3)_2$ favours nucleophilic displacement at C–OTf. In 2017, Wu and coworkers reported a combined ligand and solvent effect on a site-selective palladium-catalyzed carbonylation of bromoaryl triflates.[19] Their study reveals that monodentate ligands $P(n\text{Bu})Ad_2$ and $P(t\text{Bu})_3$ lead to reaction at C–Br regardless of the solvent, while bidentate ligands require specific solvents to be selective: xantphos and toluene leads to highly selective carbonylation at C–Br, while dppf and polar solvents such as DMF, DMSO and NMP achieve high selectivity at triflate.

For the oxidative addition of 4-bromoaryl triflate to $Pd(PCy_3)_2$, triflate is the exclusive site for oxidative addition in all tested solvents (Table 1, entry 4). In contrast, oxidative addition of 2-bromopyridyl-5-triflate exhibits a significant solvent effect. Oxidative addition is slightly selective for the triflate site in polar solvent mixtures (2:1), whereas the bromide site is preferred in THF (1:2) and toluene (1:7) (entry 5). Thus, increased solvent polarity consistently favours oxidative addition at C–OTf sites, even when controlling (as best as we can) for factors like added anions, Pd(0) ligation state, and divergence between 3-centered and nucleophilic displacement mechanisms.

## Conclusion

In summary, we have examined several specific solvent effects on the rate and site-selectivity of the oxidative addition of (hetero)aryl (*pseudo*)halides to $Pd(PCy_3)_2$. Based on our prior quantitative structure-reactivity studies and corresponding mechanistic hypotheses, we identified three cases where the interplay of substrate structure and solvent identity have a significant effect on oxidative addition outcomes with this system.

First, we identified 2-chloro-3-aminopyridine as an outlier substrate with respect to solvent effect on oxidative addition rate. There is a significant reduction in measured $\Delta G^{\ddagger}_{OA}$ in toluene compared to more polar solvents, which we attribute to the importance of solvent H-bond basicity ($pK_{HB}$) when H-bond donating EDGs are present on the substrate. Computational analysis revealed that intermolecular H-bonding between solvent and substrate will deactivate the adjacent C–X sites toward oxidative addition; thus, faster oxidative addition rates are observed in solvents with small $pK_{HB}$. This effect also manifests in site-selective oxidative addition for 2,6-dichloro-3-Z-pyridines. When Z = $NH_2$, NHAc, or OH, diminished selectivity for oxidative addition at $C_2$ is observed when H-bond accepting solvents are used, whereas with Z = OMe or OAc, selectivity is unperturbed within the range of conditions explored here.

Second, solvent polarity also affects oxidative addition site-selectivity for pyridine derivatives with EWG substituents. Improved $C_6/C_2$ selectivity for 2,6-dichloro-3-EWG-pyridines in polar solvents is likely due to different mechanisms operating for reactions at the two sites. Based on frontier molecular orbital symmetry, oxidative addition at $C_2$–X should proceed *via* a 3-centered mechanism, whereas reaction at $C_6$–X should proceed *via* a nucleophilic displacement mechanism. Higher $C_6$ selectivity in polar solvents is therefore consistent with solvent stabilization of the polar nucleophilic displacement transition state.

Third, we observe a consistent decrease in $\Delta G^{\ddagger}_{OA}$ for Ar–OTf substrates with increasing solvent polarity that is larger in magnitude for all other substrate classes studied. Hammett analysis combined with prior computational results are consistent with these substrates undergoing a polar nucleophilic displacement mechanism. Comparing the calculated transition states for the oxidative addition of 2-chloropyridine and 2-pyridyl triflate to $Pd(PCy_3)_2$ revealed that the latter is more polar than the former, with greater charge separation between Pd and the pyridyl unit. Solvent effects on triflate/halide site-selectivity for a group of 2-halopyridyl triflates are also consistent with highly polar transition states for C–OTf oxidative addition. Improved selectivity for oxidative addition at triflate occurs in polar solvents, even when the halide site is highly reactive.

Further work is underway to better quantify and predict these different solvent effects on oxidative addition for a wider range of palladium(0) species, and to elucidate the corresponding mechanistic implications. These studies will be reported in due course.

## Supporting Information

Detailed experimental procedures, characterization data, and data tables, computational methods, and tables of molecular descriptors (PDF). Coordinate files for all calculated structures (xyz in zip folder). The authors have cited additional references within the Supporting Information.[69-82]

## Acknowledgements

We acknowledge and respect the Lekwungen peoples on whose traditional territory the University of Victoria (UVic) stands, and the Songhees, Esquimalt and WSÁNEĆ peoples whose historical relationships with the land continue to this day. We also acknowledge funding from the New Frontiers in Research Fund – Exploration and the NSERC Discovery Grant programs. D.C.L. thanks the Research Corporation for Science Advancement for a Cottrell Scholar Award.

**Keywords:** organopalladium • oxidative addition • solvent effects • cross-coupling • regioselectivity

[1] E. Cesarotti, R. Ugo, L. Kaplan, *Coord. Chem. Rev.* **1982**, *43*, 275–298.
[2] T. Welton, *Chem. Rev.* **1999**, *99*, 2071–2084.
[3] J. P. Hallett, T. Welton, *Chem. Rev.* **2011**, *111*, 3508–3576.
[4] C. Reichardt, *Org. Process Res. Dev.* **2007**, *11*, 105–113.
[5] *Solvents and Solvent Effects in Organic Chemistry*, (Eds.: C. Reichardt, T. Welton), WILEY-VCH Verlag GmbH & Co. KGaA, Weinheim, **2010**.
[6] P. J. Dyson, P. G. Jessop, *Catal. Sci. Technol.* **2016**, *6*, 3302–3316.
[7] F. Huxoll, F. Jameel, J. Bianga, T. Seidensticker, M. Stein, G. Sadowski, D. Vogt, *ACS Catal.* **2021**, *11*, 590–594.
[8] Y. Hatanaka, T. Hiyama, *J. Am. Chem. Soc.* **1990**, *112*, 7793–7794.
[9] K. Ohrai, K. Kondo, M. Sodeoka, M. Shibasaki, *J. Am. Chem. Soc.* **1994**, *116*, 11737–11748.
[10] C. Yang, H. M. Lee, S. P. Nolan, *Org. Lett.* **2001**, *3*, 1511–1514.
[11] N. P. Grimster, C. Gauntlett, C. R. A. Godfrey, M. J. Gaunt, *Angew. Chem. Int. Ed.* **2005**, *44*, 3125–3129.
[12] G. Cainelli, P. Galletti, D. Giacomini, *Chem. Soc. Rev.* **2009**, *38*, 990–1001.
[13] J. C. Cárdenas, L. Fadini, C. A. Sierra, *Tet. Lett.* **2010**, *51*, 6867–6870.
[14] F. Proutiere, F. Schoenebeck, *Angew. Chem. Int. Ed.* **2011**, *50*, 8192–8195.
[15] F. Proutiere, F. Schoenebeck, *Synlett* **2012**, *23*, 645–648.
[16] S. A. Katsyuba, E. E. Zvereva, N. Yan, X. Yuan, Y. Kou, P. J. Dyson, *ChemPhysChem* **2012**, *13*, 1781–1790.
[17] X. Yuan, N. Yan, S. A. Katsyuba, E. E. Zvereva, Y. Kou, P. J. Dyson, *Phys. Chem. Chem. Phys.* **2012**, *14*, 6026–6033.
[18] X. Marset, A. Khoshnood, L. Sotorríos, E. Gómez-Bengoa, D. A. Alonso, D. J. Ramón, *ChemCatChem* **2017**, *9*, 1269–1275.
[19] C. Shen, Z. Wei, H. Jiao, X.-F. Wu, *Chem. Eur. J.* **2017**, *23*, 13369–13378.
[20] J. J. Varghese, S. H. Mushrif, *React. Chem. Eng.* **2019**, *4*, 165–206.
[21] E. K. Elias, S. M. Rehbein, S. R. Neufeldt, *Chem. Sci.* **2022**, *13*, 1618–1628.
[22] J. Sherwood, J. H. Clark, I. J. S. Fairlamb, J. M. Slattery, *Green Chem.* **2019**, *21*, 2164–2213.
[23] E. K. Reeves, O. R. Bauman, G. B. Mitchem, S. R. Neufeldt, *Isr. J. Chem.* **2020**, *60*, 406–409.
[24] M. C. D'Alterio, È. Casals-Cruañas, N. V. Tzouras, G. Talarico, S. P. Nolan, A. Poater, *Chem. Eur. J.* **2021**, *27*, 13481–13493.
[25] M. H. Abraham, in *Progress in Physical Organic Chemistry*, Vol. 11 (Eds.: A. Streitwieser Jr., R. W. Taft), John Wiley & Sons, New York, London, Sydney, Toronto, **1974**, pp. 1–87.
[26] E. Paenurk, K. Kaupmees, D. Himmel, A. Kütt, I. Kaljurand, I. A. Koppel, I. Krossing, I. Leito, *Chem. Sci.* **2017**, *8*, 6964–6973.
[27] M. Lõkov, S. Tshepelevitsh, A. Heering, P. G. Plieger, R. Vianello, I. Leito, *Eur. J. Org. Chem.* **2017**, *2017*, 4475–4489.
[28] S. Tshepelevitsh, A. Kütt, M. Lõkov, I. Kaljurand, J. Saame, A. Heering, P. G. Plieger, R. Vianello, I. Leito, *Eur. J. Org. Chem.* **2019**, *2019*, 6735–6748.
[29] T. Diao, P. White, I. Guzei, S. S. Stahl, *Inorg. Chem.* **2012**, *51*, 11898–11909.
[30] J. A. Molina de la Torre, P. Espinet, A. C. Albéniz, *Organometallics* **2013**, *32*, 5428–5434.
[31] J. K. Stille, K. S. Y. Lau, *Acc. Chem. Res.* **1977**, *10*, 434–442.
[32] C. Amatore, A. Jutand, *Coord. Chem. Rev.* **1998**, *178–180*, 511–528.
[33] J. A. Labinger, *Organometallics* **2015**, *34*, 4784–4795.
[34] J. Rio, H. Liang, M.-E. L. Perrin, L. A. Perego, L. Grimaud, P.-A. Payard, *ACS Catal.* **2023**, *13*, 11399–11421.
[35] F. Barrios-Landeros, B. P. Carrow, J. F. Hartwig, *J. Am. Chem. Soc.* **2009**, *131*, 8141–8154.
[36] E. A. Mitchell, P. G. Jessop, M. C. Baird, *Organometallics* **2009**, *28*, 6732–6738.
[37] J. Lu, H. Celuszak, I. Paci, D. C. Leitch, *ChemRxiv*, **2024**, DOI:
[38] M. J. Kamlet, R. W. Taft, *J. Am. Chem. Soc.* **1976**, *98*, 377–383.
[39] J. Lu, N. D. Schley, I. Paci, D. C. Leitch, *ChemRxiv* **2024**, DOI: 10.26434/chemrxiv-2024-lrdz4-v2.
[40] F. Schoenebeck, K. N. Houk, *J. Am. Chem. Soc.* **2010**, *132*, 2496–2497.
[41] M. J. Kania, A. Reyes, S. R. Neufeldt, *ChemRxiv* **2024**, DOI: 10.26434/chemrxiv-2024-h2s9s-v2.
[42] J.-F. Fauvarque, F. Pflüger, M. Troupel, *J .Organomet. Chem.* **1981**, *208*, 419–427.
[43] C. L. McMullin, J. Jover, J. N. Harvey, N. Fey, *Dalton Trans.* **2010**, *39*, 10833–10836.
[44] M. Portnoy, D. Milstein, *Organometallics* **1993**, *12*, 1665–1673.
[45] A. Ariafard, Z. Lin, *Organometallics* **2006**, *25*, 4030–4033.
[46] B. U. W. Maes, S. Verbeeck, T. Verhelst, A. Ekomié, N. von Wolff, G. Lefèvre, E. A. Mitchell, A. Jutand, *Chem. Eur. J.* **2015**, *21*, 7858–7865.
[47] J. P. Norman, N. G. Larson, S. R. Neufeldt, *ACS Catal.* **2022**, *12*, 8822–8828.
[48] J. Lu, S. Donnecke, I. Paci, D. C. Leitch, *Chem. Sci.* **2022**, *13*, 3477–3488.
[49] *The Hydrogen Bond: Recent Developments in Theory and Experiments*, (Eds.: P. Schuster, G. Zundel, C. Sandorfy), North-Holland Publishing Company, Amsterdam, New York, Oxford, **1976**.
[50] A. G. Doyle, E. N. Jacobsen, *Chem. Rev.* **2007**, *107*, 5713–5743.
[51] C. Laurence, K. A. Brameld, J. Graton, J.-Y. Le Questel, E. Renault, *J. Med. Chem.* **2009**, *52*, 4073–4086.
[52] V. Amendola, L. Fabbrizzi, L. Mosca, *Chem. Soc. Rev.* **2010**, *39*, 3889–3915.
[53] S. J. Grabowski, *Chem. Rev.* **2011**, *111*, 2597–2625.
[54] C. N. Pace, H. Fu, K. Lee Fryar, J. Landua, S. R. Trevino, D. Schell, R. L. Thurlkill, S. Imura, J. M. Scholtz, K. Gajiwala, J. Sevcik, L. Urbanikova, J. K. Myers, K. Takano, E. J. Hebert, B. A. Shirley, G. R. Grimsley, *Prot. Sci.* **2014**, *23*, 652–661.
[55] M.-X. Du, Y.-F. Yuan, J.-M. Zhang, C.-Y. Liu, *Macromolecules* **2022**, *55*, 4578–4588.
[56] J. N. H. Reek, B. de Bruin, S. Pullen, T. J. Mooibroek, A. M. Kluwer, X. Caumes, *Chem. Rev.* **2022**, *122*, 12308–12369.
[57] G. Pupo, V. Gouverneur, *J. Am. Chem. Soc.* **2022**, *144*, 5200–5213.
[58] X. Wang, E. J. Salaski, D. M. Berger, D. Powell, *Org. Lett.* **2009**, *11*, 5662–5664.
[59] J. Ruan, J. A. Iggo, N. G. Berry, J. Xiao, *J. Am. Chem. Soc.* **2010**, *132*, 16689–16699.
[60] See the Supporting Information for more details.
[61] S. R. Gadre, C. H. Suresh, N. Mohan, *Molecules* **2021**, *26*, 3289.
[62] Note that our quantitative prediction models underestimate the magnitude of site-selectivity for these 2,6-dichloropyridines. See ref. [39].
[63] A. Jutand, A. Mosleh, *Organometallics* **1995**, *14*, 1810–1817.
[64] R. P. Bell, *Proc. Royal Soc. London A – Math. Phys. Sci.* **1936**, *154*, 414–429.
[65] M. G. Evans, M. Polanyi, *Trans. Faraday Soc.* **1936**, *32*, 1333–1360.
[66] A. F. Littke, C. Dai, G. C. Fu, *J. Am. Chem. Soc.* **2000**, *122*, 4020–4028.
[67] Z. L. Niemeyer, A. Milo, D. P. Hickey, M. S. Sigman, *Nat. Chem.* **2016**, *8*, 610–617.
[68] J. Wang, M. A. Seefeld, J. Luengo, *Tet. Lett.* **2011**, *52*, 6346–6348.